Article

Formation and Characterization of Self-Organized TiO Nanotube Arrays by Pulse Anodization

Wilaiwan Chanmanee, Apichon Watcharenwong, C. Ramannair Chenthamarakshan, Puangrat Kajitvichyanukul, Norma R. de Tacconi, and Krishnan Rajeshwar

J. Am. Chem. Soc., **2008**, 130 (3), 965-974 • DOI: 10.1021/ja076092a

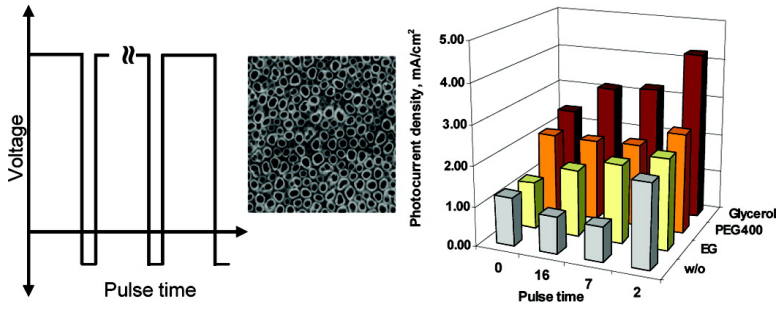

More About This Article

Additional resources and features associated with this article are available within the HTML version:

- Supporting Information
- Links to the 3 articles that cite this article, as of the time of this article download
- Access to high resolution figures
- Links to articles and content related to this article
- Copyright permission to reproduce figures and/or text from this article

View the Full Text HTML

J|A|C|S
ARTICLES
Published on Web 12/29/2007

Formation and Characterization of Self-Organized TiO_2 Nanotube Arrays by Pulse Anodization

Wilaiwan Chanmanee,[†] Apichon Watcharenwong,[†]
C. Ramannair Chenthamarakshan,[‡] Puangrat Kajitvichyanukul,[§]
Norma R. de Tacconi,*[,‡] and Krishnan Rajeshwar*[,‡]

National Research Center for Environmental and Hazardous Waste Management, Chulalongkorn University, Bangkok, Thailand, Center for Renewable Energy Science and Technology (CREST), Department of Chemistry and Biochemistry, The University of Texas at Arlington, Arlington, Texas 76019, and Department of Environmental Engineering, Faculty of Engineering, King Mongkut's University of Technology Thonburi, Bangkok, Thailand

Received August 13, 2007; E-mail: rajeshwar@uta.edu; ntacconi@uta.edu

Abstract: This paper describes TiO_2 nanotube arrays prepared by anodic oxidation of Ti substrates using pulse voltage waveforms. Voltages were pulsed between 20 and −4 V or between 20 and 0 V with varying durations from 2 to 16 s at the lower limit of the pulse waveform. Ammonium fluoride or sodium fluoride (and mixtures of both) was used as the electrolyte with or without added medium modifier (glycerol, ethylene glycol, or poly (ethylene glycol) (PEG 400)) in these experiments. The pulse waveform was optimized to electrochemically grow TiO_2 nanotubes and chemically etch their walls during its cathodic current flow regime. The resultant TiO_2 nanotube arrays showed a higher quality of nanotube array morphology and photoresponse than samples grown via the conventional continuous anodization method. Films grown with a 20 V/−4 V pulse sequence and pulse duration of 2 s at its negative voltage limit afforded a superior photoresponse compared to other pulse durations. Specifically, the negative voltage limit of the pulse (−4 V) and its duration promote the adsorption of NH_4^+ species that in turn inhibits chemical attack of the growing oxide nanoarchitecture by the electrolyte F^- species. The longer the period of the pulse at the negative voltage limit, the thicker the nanotube walls and the shorter the nanotube length. At variance, with 0 V as the low voltage limit, the longer the pulse duration, the thinner the oxide nanotube wall, suggesting that chemical attack by fluoride ions is not counterbalanced by NH_3/NH_4^+ species adsorption, unlike the interfacial situation prevailing at −4 V. Finally, the results from this study provide useful evidence in support of existing mechanistic models for anodic growth and self-assembly of oxide nanotube arrays on the parent metal surface.

Introduction

This paper elaborates on a recent communication[1] from our laboratories that illustrates the utility of employing a pulse waveform for the anodic growth of titanium dioxide (TiO_2) nanotube arrays. There is growing interest, from both fundamental and practical perspectives, in the anodic growth of TiO_2 nanotube arrays on titanium substrate.[1−15] Nanotubes fabricated by this method are highly ordered, have high aspect ratios, and are oriented perpendicular to the substrate. Oxide formation and nanotube self-assembly are afforded by a fine balance between the electrochemical processes (field-assisted oxide growth and metal etching) and chemical dissolution of the substrate by the presence of an acidic or complex-forming electrolyte.[3,16−18] When electrochemical growth proceeds faster than the chemical dissolution, the barrier layer increases, which in turn reduces the electrochemical etch process, and thus the chemical dissolution is the determining factor in the oxide self-assembly.

[†] Chulalongkorn University.
[‡] The University of Texas at Arlington.
[§] King Mongkut's University of Technology Thonburi.

(1) Chanmanee, W.; Watcharenwong, A.; Chenthamarakshan, C. R.; Kajitvichyanukul, P.; de Tacconi, N. R.; Rajeshwar, K. *Electrochem. Commun.* **2007**, *9*, 2145.
(2) Gong, D.; Grimes, C. A.; Varghese, O. K.; Hu, W.; Singh, R. S.; Chen, Z.; Dickey, E. C. *J. Mater. Res.* **2001**, *16*, 3331.
(3) Review: Mor, G. K.; Oomman, K. V.; Paulose, M.; Shankar, K.; Grimes, C. A. *Sol. Energy Mater. Sol. Cells* **2006**, *90*, 2011 and also references therein.
(4) Shankar, K.; Mor, G. K.; Prakasam, H. E.; Yoriya, S.; Paulose, M.; Varghese, O. K.; Grimes, C. A. *Nanotechnology* **2007**, *18*, 065707.
(5) Beranek, R.; Hildebrand, H.; Schmuki, P. *Electrochem. Solid-State Lett.* **2003**, *6*, B12.
(6) Macak, J. M.; Tsuchiya, H.; Taveira, L.; Aldabergerwa, S.; Schmuki, P. *Angew. Chem., Int. Ed.* **2005**, *44*, 7463.
(7) Macak, J. M.; Schmuki, P. *Electrochim. Acta* **2006**, *52*, 1258.
(8) Macak, J. M.; Taveira, L. V.; Tsuchiya, H.; Sirotna, K.; Macak, J.; Schmuki, P. *J. Electroceram.* **2006**, *16*, 29.
(9) Raja, K. S.; Misra, M.; Paramguru, K. *Electrochim. Acta* **2005**, *51*, 154.
(10) Mohapatra, S.; Misra, M.; Mahajan, V. K.; Raja, K. S. *J. Phys. Chem. C* **2007**, *111*, 8677. See also references therein.
(11) Zhao, J.; Wang, X.; Chen, R.; Li, L. *Solid State Commun.* **2005**, *134*, 705.
(12) Zhao, J.; Wang, X.; Sun, T.; Li, L. *Nanotechnology* **2005**, *16*, 2450.
(13) Xie, Y.; Zhou, L. M.; Huang, H. *Mater. Lett.* **2006**, *60*, 3558.
(14) de Tacconi, N. R.; Chenthamarakshan, C. R.; Yogeeswaran, G.; Watcharenwong, A.; de Zoysa, S.; Basit, N. A.; Rajeshwar, K. *J. Phys. Chem. B* **2006**, *110*, 25347.
(15) Kaneco, S.; Chen, Y.; Westerhoff, P.; Crittenden, J. C. *Scr. Mater.* **2007**, *56*, 373.
(16) Lehmann, V.; Göselle, U. *Appl. Phys. Lett.* **1991**, *58*, 856.
(17) Jessensky, O.; Muller, F.; Göselle, U. *Appl. Phys. Lett.* **1998**, *72*, 1173.
(18) Zwilling, V.; Aucouturier, M.; Darque-Ceretti, E. *Electrochim. Acta* **1991**, *44*, 921.

However the nanotubes cannot be formed if the chemical dissolution is too high or too low which results in either rapid or very slow oxide formation.

Previous anodization studies, including our own,[2−15] have used either constant potential (potentiostatic) or constant current (galvanostatic) nanotube growth modes. In this paper, pulse anodization is shown to result in better-defined nanotube morphologies than in the constant voltage growth mode. The resultant TiO_2 nanotube arrays show a higher quality of photoresponse than those grown via the continuous anodization route. Important mechanistic insights are also furnished by these data. Careful tuning of the pulse duty cycle and the negative voltage limit point toward the importance of *chemical* (corrosion) processes during nanotube growth as well as surface passivation effects introduced by the adsorption of electrolyte species (e.g., NH_4^+) on the growing oxide nanotube arrays. From a practical process economics perspective, it is worth noting that pulse anodization also offers savings in energy consumption relative to the continuous process counterpart. Previous authors do report[19] the use of positive voltage pulses for oxide film growth on valve metal substrates, but in this particular study, very high voltage (>1000 V) pulses were used and no nanotube formation was noted.

Materials and Methods

Preparation of TiO_2 Nanotubes. The titanium foils (99.95%, Alfa Aesar) were 0.25 mm thick. They were polished to a mirror quality smooth finish using silicon carbide sandpaper of successively finer roughness (220, 240, 320, 400, 600, 800, 1000, and 1500 grit) and degreased by successively sonicating for 5 min in acetone, isopropanol, and finally ultrapure water. They were then dried under a flowing N_2 stream and used immediately.

For the anodic growth experiments, the titanium foil was contacted and then pressed against an O-ring in an electrochemical cell, leaving 0.63 cm^2 exposed to the electrolyte.[14] A two-electrode configuration was used for anodization. Titanium foil ($14 \times 14 \times 0.25$ mm^3) was used as the anode while a large platinum coil was used as the cathode. Anodization experiments were carried out using a multioutput power supply (Switching System International, CA) connected to a digital multimeter. For the pulse anodization treatment, a square waveform shown in Figure 1a was employed. Voltages were pulsed between 20 and 0 V or between 20 V and −4 V. The positive voltage limit of the pulse was fixed at 20 V since it provided the best results for nanotube morphology using the conventional anodization approach.[1,14] The pulse duration (t_1 ~3 min) at the anodic limit was set longer than the pulse duration (t_0) at the lower potential of the waveform, with t_0 adjusted between 2 and 30 s. Films were grown for 3 h and compared to those obtained at constant voltage (20 V) for the same period of time.

All films were grown at room temperature (25 ± 2 °C) and from 0.36 M NH_4F electrolyte without and with medium modifiers, namely glycerol, poly (ethylene glycol) (PEG 400) or ethylene glycol. Solutions were prepared from reagent grade chemicals and deionized water (18 MΩ cm). After formation of the oxide, the anodized Ti foil was removed from the O-ring assembly and carefully washed by immersion in deionized water and then dried in a flowing N_2 stream. The as-grown porous layers were annealed at 450 °C for 30 min in a furnace (model 650-14 Isotemp Programmable Muffle Furnace, Fisher Scientific) and were allowed to cool gradually back to the ambient condition. The anneal consisted of a liner heat ramp (at 25 °C/min) from room temperature to a final temperature of 450 °C. This protocol was designed to decompose any organic residue from the adsorbed (see below) polyhydric alcohol used in the bath for film preparation. For instance, PEG begins to thermally decompose at ~250 °C.[20]

Photoelectrochemical Measurements and Characterization. A standard single-compartment, three-electrode electrochemical cell was used for the photoelectrochemical measurements. A Pt foil ($10 \times 25 \times 0.1$ mm^3) and a Ag|AgCl|satd. KCl reference electrode completed the cell setup. The UV light source was a 150 W xenon arc lamp (Oriel, Stratford, CT), and the nominal incident photon flux was 0.59 mW/cm^2 at 340 nm (bandwidth: 4 nm). Photovoltammetry profiles were recorded on a model CV-27 Voltammograph (Bioanalytical Systems, West Lafayette, IN) equipped with a model VP-6414S Soltec X-Y recorder in 0.5 M Na_2SO_4 electrolyte. The photovoltammogram scans were obtained using a slow potential sweep (2 mV/s) in conjunction with interrupted irradiation (0.1 Hz) of the semiconductor film. The morphology and microstructure of the nanotubes were observed on a scanning electron microscope (Zeiss Supra 55) with a nominal electron beam voltage of 5 kV. Raman spectra were recorded with a Horiba Jobin Yvon LabRam ARAMIS instrument using an excitation wavelength of 473 nm and a 600 line/mm grating. In all the cases the slit width was 10 μm, and 10 scans were accumulated for each spectrum. Spectra were obtained for TiO_2 nanotube arrays after thermal anneal and after contact with the preparative electrolytic bath.

Results and Discussion

In a previous paper, we reported the anodic growth of self-organized nanoporous TiO_2 films by anodization under different conditions.[14] From this work it was obvious that the nanotube morphology, tube diameter, wall thickness, and photocurrent response depended on the anodization and growth medium variables. In the present study, we expand the anodization protocol to a wider range of growth conditions as shown in Table 1. The nanotube arrays are now grown from Ti foils by pulse anodization using either 20 V/−4 V or 20 V/0 V sequences. In either case, the potential perturbation was applied for 3 h and compared to films prepared for the same time period but under constant polarization, i.e., at 20 V. The pulse durations were set in the 150−180 s range for the positive potential limit and in the 2−30 s for the lower potential pulse. Table 1 compiles the potentials and pulse durations combined with four electrolyte compositions. Moderately concentrated NH_4F (0.36 M) was used as both a supporting electrolyte and chemical complexing agent; it was used directly in aqueous solution (entries no. 1−8 in Table 1) or in combination with a medium modifier; i.e., dissolved in 90% glycerol/10% water (entries no. 9−16), in 90% ethylene glycol/10% water (entries no. 17−24), and in 80% PEG 400/20% water (entry nos. 25−32).

Effect of Pulse Anodization. The scanning electron microscopy (SEM) images in Figure 2 compare the surface morphology of TiO_2 films prepared by conventional anodization (20 V, 3 h) in 0.36 M NH_4F and 0. 36 M NH_4F/glycerol−H_2O (90:10) electrolytes (Figure 2a and c) and pulse anodization using a 20 V/−4 V pulse sequence for 2 s in the same electrolytes (Figure 2b and d).

The organic additive was intentionally omitted for the films shown in Figure 2a and b to bring out the effect of glycerol on the ordering of the anodic layer nanoarchitecture. Glycerol was reported by other authors[6] to exert a viscosity modifying effect to afford smooth TiO_2 nanotubes by suppressing local concentration fluctuations and pH bursts during anodization. However, a comparison of Figure 2b and d immediately reveals that, even

(19) Poznyak, S. K.; Talapin, D. V.; Kulak, A. I. *J. Electroanal. Chem.* **2005**, *579*, 299.

(20) Matsuda, A.; Katayarna, S.; Tsuno, T.; Tohge, N.; Minami, T. *J. Am. Ceram. Soc.* **1990**, *75*, 2217.

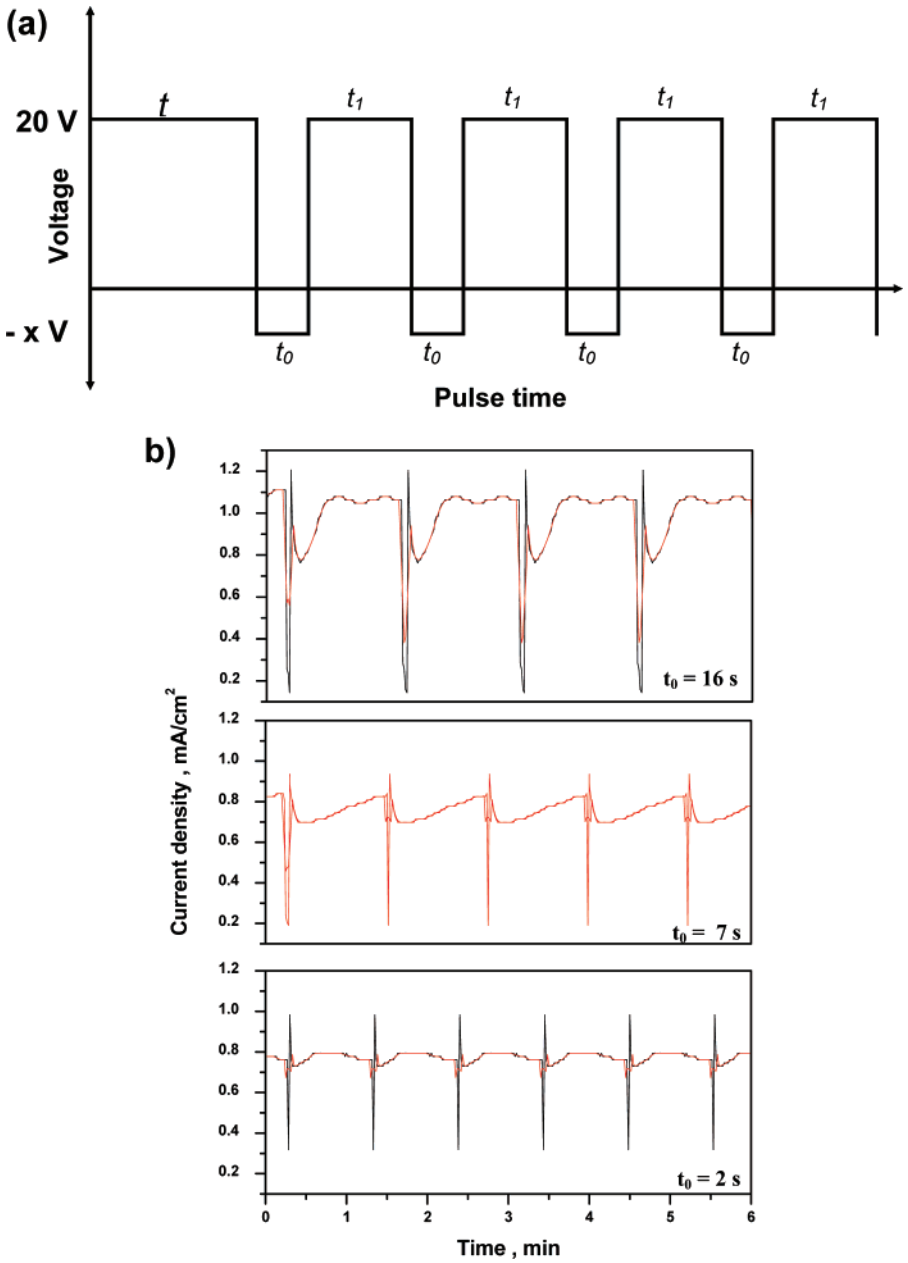

Figure 1. (a) Schematic representation of the voltage−time waveform for pulse anodization. An initial constant time of $t = 5$ min was applied at 20 V, and then the pulse wave form is applied with time t_0 and t_1 (s) values as shown in Table 1. (b) Current density vs time recorded on a Ti foil with a 20 V/0 V pulse waveform adjusted at pulse durations of 16, 7, and 2 s at its lower voltage limit. Electrolyte: 0.36 M NH_4F in ethylene glycol/water (90:10).

under the supposedly "adverse" conditions in the absence of this organic additive, the pulse anodization approach affords a self-ordered array of TiO_2 nanotubes on the Ti substrate. The nanotube array morphology is considerably improved when pulse anodization is combined with organic additive addition to the electrolyte (Figure 2d). Importantly, TiO_2 nanotubes grown in aqueous NH_4F using the pulse anodization mode is seen to result in better-defined nanotube morphologies than those in the constant voltage growth mode (cf., Figure 2a and c).

The average inner nanotube diameter increases from 68 ± 2 nm to 83 ± 2 nm with a pulsing protocol involving a 2 s duration at the negative voltage (Figure 2c and d). This enlargement trend is accompanied by a thickening of the nanotube walls which are seen to grow from 13.0 ± 0.5 nm to 15.6 ± 0.5 nm. Thicker walls are obtained if the duration of the negative potential limit is increased (see Table 1). Thus, Figure 3 shows the changes in the nanotube wall thickness (Figure 3a) and diameter (Figure 3b) as a function of the duration of the pulse (t_0) at the lower potential of the waveform. Data in this figure are for a 20V/−4V waveform. The range of wall thickening dimensions depends on the composition of the electrolyte, i.e., is higher in PEG 400 than in glycerol or ethylene glycol, but in all the three cases, a systematic increase is observed when t_0 is increased. These findings point to NH_4^+ and F^- (which are present at the same concentration in the three cases studied) as the possible chemical culprits for these effects.

Another finding was that the nanotubes prepared by pulse anodization were shorter than those under constant voltage (see Table 1). As an example, in the nanotube arrays prepared from glycerol/H_2O 90:10 with 20 V/−4 V pulse anodization, a decrease in length from 580 ± 10 nm to 390 ± 10 nm was observed when t_0 was increased from 2 to 30 s. Two factors

Table 1. Anodization Conditions, Photoelectrochemical Performance, and Morphology of TiO_2 Nanotube Films in This Study

entry no.	electrolyte, medium modifier	duration of pulse anodization (t_1, t_0)	pulse anodization voltage, time	nanotube length[a] (nm)	wall thickness[a] (nm)	nanotube diameter[a] (nm)	j_{ph}[b] (mA cm^{-2})
1	0.36 M NH_4F	-	20 V, 3 h	n.d.[c]	n.d	n.d.	1.2 ± 0.2
2	”	150, 2 s	20 V/−4 V, 3 h	2090 ± 10	n.d.	n.d.	2.1 ± 0.1
3	”	160, 7 s	20 V/−4 V, 3 h	n.d.	n.d.	n.d.	0.9 ± 0.2
4	”	170, 16 s	20 V/−4 V, 3 h	n.d.	n.d.	n.d.	0.8 ± 0.1
5	”	180, 30 s	20 V/−4 V, 3 h	300 ± 10	19.0 ± 0.5	67 ± 2	2.0 ± 0.1
6	”	150, 2 s	20 V/0 V, 3 h	n.d.	n.d.	n.d.	1.7 ± 0.2
7	”	160, 7 s	20 V/0 V, 3 h	n.d.	n.d.	n.d.	1.4 ± 0.1
8	”	170, 16 s	20 V/0 V, 3 h	n.d.	n.d.	n.d.	1.5 ± 0.1
9	0.36 M NH_4F/ glycerol−H_2O (90:10)	-	20 V, 3 h	600 ± 10	13.0 ± 0.5	68 ± 2	1.6 ± 0.2
10	”	150, 2 s	20 V/−4 V, 3 h	580 ± 10	15.6 ± 0.5	83 ± 2	4.2 ± 0.1
11	”	160, 7 s	20 V/−4 V, 3 h	n.d.	16.4 ± 0.5	70 ± 2	3.2 ± 0.1
12	”	170, 16 s	20 V/−4 V, 3 h	480 ± 10	17.9 ± 0.5	76 ± 2	3.1 ± 0.2
13	”	180, 30 s	20 V/−4 V, 3 h	390 ± 10	20.6 ± 0.5	60 ± 2	2.1 ± 0.1
14	”	150, 2 s	20 V/0 V, 3 h	n.d.	11.2 ± 0.5	72 ± 2	3.7 ± 0.1
15	”	160, 7 s	20 V/0 V, 3 h	n.d.	15.6 ± 0.5	73 ± 2	2.6 ± 0.2
16	”	170, 16 s	20 V/0 V, 3 h	230 ± 10	13.4 ± 0.5	72 ± 2	2.2 ± 0.1
17	0.36 M NH_4F/ethylene glycol−H_2O (90:10)	-	20 V, 3 h	835 ± 10	14.4 ± 0.6	55 ± 3	1.2 ± 0.2
18	”	150, 2 s	20 V/−4 V, 3 h	n.d.	15.4 ± 0.5	82 ± 2	2.3 ± 0.2
19	”	160, 7 s	20 V/−4 V, 3 h	n.d.	15.8 ± 0.5	78 ± 2	2.0 ± 0.1
20	”	170, 16 s	20 V/−4 V, 3 h	n.d.	16.6 ± 0.5	70 ± 2	1.7 ± 0.1
21	”	180, 30 s	20 V/−4 V, 3 h	n.d.	17.4 ± 0.5	62 ± 2	1.3 ± 0.1
22	”	150, 2 s	20 V/0 V, 3 h	525 ± 10	14.3 ± 0.6	69 ± 1	1.8 ± 0.1
23	”	160, 7 s	20 V/0 V, 3 h	435 ± 10	12.6 ± 0.6	70 ± 2	1.8 ± 0.2
24	”	170, 16 s	20 V/0 V, 3 h	365 ± 10	11.2 ± 0.6	71 ± 2	1.7 ± 0.1
25	0.36 NH_4F/PEG400− H_2O (80:20)	-	20 V, 3 h	725 ± 10	16.0 ± 0.4	120 ± 3	2.1 ± 0.2
26	”	150, 2 s	20 V/−4 V, 3 h	n.d.	15.4 ± 0.5	123 ± 2	2.5 ± 0.1
27	”	160, 7 s	20 V/−4 V, 3 h	n.d.	17.9 ± 0.5	120 ± 2	2.1 ± 0.1
28	”	170, 16 s	20 V/−4 V, 3 h	n.d.	20.1 ± 0.5	116 ± 2	2.1 ± 0.1
29	”	180, 30 s	20 V/−4 V, 3 h	n.d.	21.2 ± 0.5	104 ± 2	2.0 ± 0.1
30	”	150, 2 s	20 V/0 V, 3 h	n.d.	16.1 ± 0.4	91 ± 2	2.4 ± 0.2
31	”	160, 7 s	20 V/0 V, 3 h	n.d.	12.7 ± 0.4	92 ± 2	2.1 ± 0.1
32	”	170, 16 s	20 V/0 V, 3 h	n.d.	11.3 ± 0.5	93 ± 2	2.0 ± 0.2

[a] As assessed by SEM. [b] j_{ph} = photocurrent density in 0.5 M Na_2SO_4 at 1.5 V. [c] No data available.

are likely coupled for the decrease of the nanotube length with the pulse duration at the lower potential: (a) When the walls grow thicker, they contain more material in the $x-y$ plane and therefore the z-axis (nanotube length) should be shorter than in the case of thinner walls in order to maintain the same amount of TiO_2 in both cases. (b) The pulse anodization was applied for the same total time of 3 h as in the case of the constant voltage anodization; therefore the time for the growth of the nanotubes at the positive potential limit is shorter in the first case than in the second. For instance, with a cathodic pulse duration of 30 s, the *real* time for anodization is in fact 2 h 30 min instead of 3 h as is the case of the constant voltage anodization mode. We intentionally kept the total time constant to bring out the benefits in the photoelectrochemical quality of the films prepared by pulse anodization vs the conventional anodization. Importantly, when the lower pulse limit is set at 0 V, both nanotube wall thickness and nanotube length decrease (see Table 1). These results demonstrate that, at 0 V, the main effect is that of fluoride ions at the outer interface (oxide/electrolyte) that dissolve the TiO_2 surface by formation of highly soluble TiF_6^{2-} (see below).

It is worth noting that long t_0 periods promote the increase of the barrier layer that in turn decreases the growth rate of the nanotube array. This is a shortcoming in any application where the length of the nanotube arrays is an important variable related to their performance, but not for those applications using UV excitation light in that the arrays are longer than the depth of light penetration (α^{-1}) into the film. As an example, a wavelength of 340 nm will have a light penetration depth (L_λ) of only 200 nm[21] while at 335 nm the L_λ value will be ∼100 nm.[22] In both cases the light penetration depth corresponds to the inverse of the absorption coefficient, α, of the anatase TiO_2 phase.[21,22]

The nanotube walls are thicker in the 20 V/−4 V pulse anodized films than those prepared by constant anodization, indicating that these films contain a larger amount of TiO_2 per unit length. This trend is not observed when a 20 V/0 V pulse perturbation is used in any of the four electrolytic media (see Table 1). The negative limit of the voltage pulse (Figure 1a) and the related current transient in the pulse regime (Figure 1b) both exert a crucial effect on the nanotube morphology mainly controlled by the following chemical and electrochemical reactions (eqs 1 and 2):

$$TiO_2 + 6NH_4F \rightarrow TiF_6^{2-} + 6NH_3 + 2H_2O + 2H^+ \quad (1)$$

$$2H^+ + 2e^- \rightarrow H_2 \quad (2)$$

(21) Mollers, F.; Tolle, H. J.; Memming, R. *J. Electrochem. Soc.* **1974**, *121*, 1160.
(22) Lindquist, S.-E.; Finnström, B.; Tegnér, L. *J. Electrochem. Soc.* **1983**, *130*, 351.

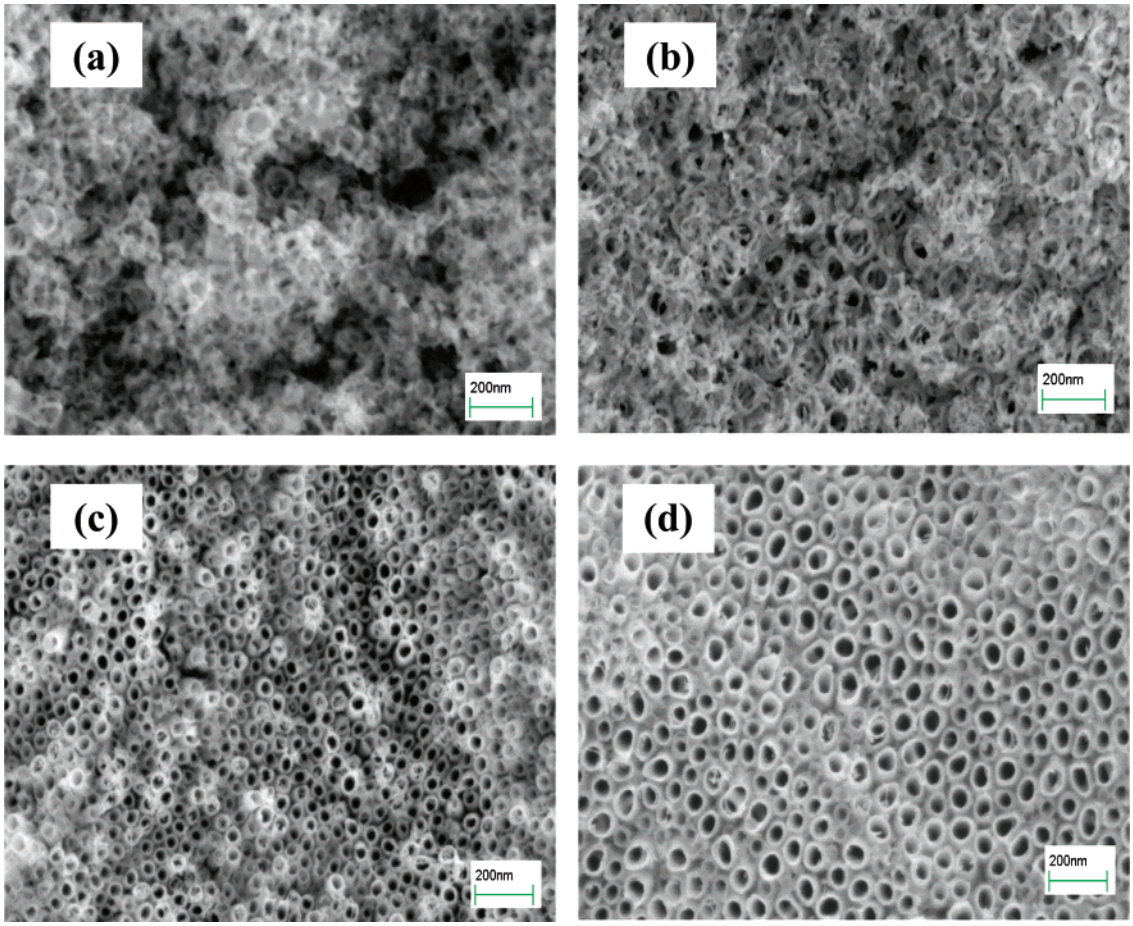

Figure 2. SEM images of TiO_2 nanotube arrays grown by conventional anodization (20 V, 3 h) (a, c) compared with corresponding samples from pulse anodization at 20 V/−4 V (2 s pulse duration at the negative voltage limit) (b, d). Frames (a) and (b) correspond to 0.36 M NH_4F electrolyte in an aqueous medium, and frames (c) and (d) correspond to the same electrolyte in a glycerol medium.

These account for the progression in layer morphology from a nanoporous structure (Figure 2a) to a discrete tubular appearance (Figure 2b) when the chemical dissolution process (eq 1) is allowed to exert its effect through the duration t_0 of the pulse at the lower voltage limit. Important to note is the fact that reaction 2 is not relevant when polyhydric alcohols are the main component of the electrolytic bath as only very little water is present to sustain the hydrogen evolution reaction.

Effect of Pulse Limits (20 V/0 V and 20 V/−4 V). Figure 4 compares the SEM morphology of TiO_2 samples prepared by pulse anodization at 20 V/0 V and 20 V/−4 V respectively. The pulse duration was 16 s in both of the cases, and films were grown in NH_4F/glycerol electrolyte (0.36 M) containing 10% water for 3 h. The TiO_2 nanotubes grown at 20 V/−4 V are thicker, and the nanotubes are longer than those grown at 20 V/0 V (see Table 1).

The four processes of nanotube growth, self-assembly, and chemical and electrochemical dissolution must be carefully balanced. In this regard, a negative voltage limit (e.g., −4 V) serves to electrostatically induce the binding of NH_4^+/NH_3 species (eq 3):

$$TiO_2 + NH_4^+ \rightarrow TiO_2(NH_4^+)_{ads} \qquad (3)$$

This interfacial process will protect the nanotube walls against chemical etch by F^- ions or at least ameliorate the extent of it. Thus, when the lower voltage limit is set at 0 V, the protection by NH_4^+ species is less versus etching by fluoride species, and the nanotube wall is slightly thinner or even not affected when compared to those prepared by constant anodization. The net result is that the samples obtained from a 20 V/0 V pulse sequence have an inferior morphology (and photoresponse quality, see below) relative to those from the 20 V/−4 V pulse mode.

Tuning of Nanotube Growth and Self-Assembly via Interfacial Chemistry and Electrochemistry. There is a corpus of both experimental[23−25] and theoretical[26,27] evidence for the adsorption of NH_3/NH_4^+ species on the TiO_2 surface. These include scanning tunneling microscopy evidence for ammonia adsorption on 5-fold coordinated Ti sites on the TiO_2 (101) surface.[24] Density functional theory calculations indicate the favored adsorption modes of both dissociated and undissociated species and the importance of H-bonding on relaxed and fixed surface oxide model clusters.[27]

To further elaborate the influence of the ammonium cation on nanotube array growth in our pulse anodization experiments, a series of films were prepared in PEG 400/H_2O (90:10) with 2, 7, and 16 s at the −4 V limit of the pulse. The electrolyte contained the same fluoride ion concentration (0.36 M) but

(23) Pittman, R. M.; Bell, A. T. *Catal. Lett.* **1994**, *24*, 1.
(24) Pang, C. L.; Sasahara, A.; Onishi, H. *Nanotechnology* **2007**, *18*, 044003/1−044003/4 (preprint online version).
(25) Roman, E.; De Segovia, J. L. *Surf. Sci.* **1991**, *742*, 251−252.
(26) Markovits, A.; Ahdjoudj, J.; Minot, C. *Surf. Sci.* **1996**, *365*, 649.
(27) Onal, I.; Soyer, S.; Senkan, S. *Surf. Sci.* **2006**, *600*, 2457−2469.

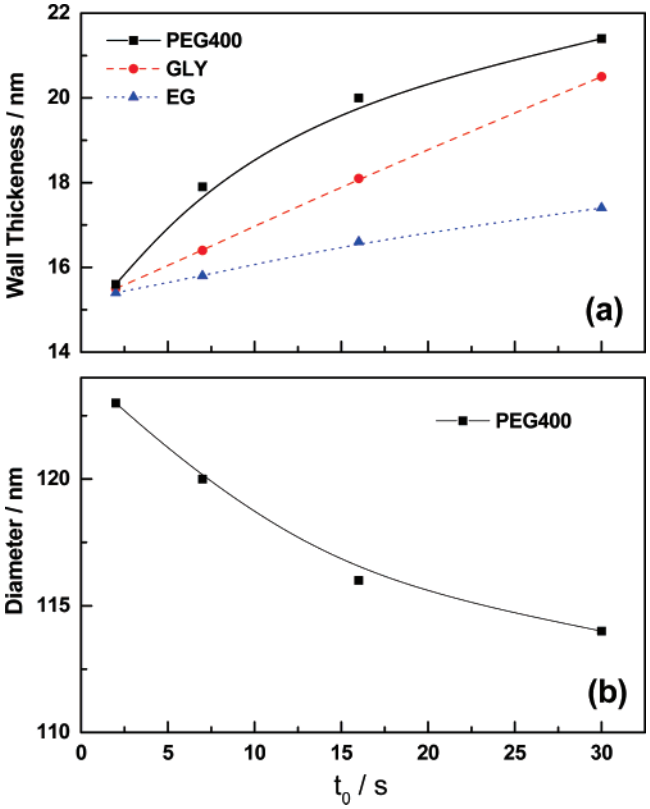

Figure 3. Nanotube wall thickness (Figure 3a) and diameter (Figure 3b) as a function of pulse duration (t_0) at the lower (i.e., more negative) potential of the waveform.

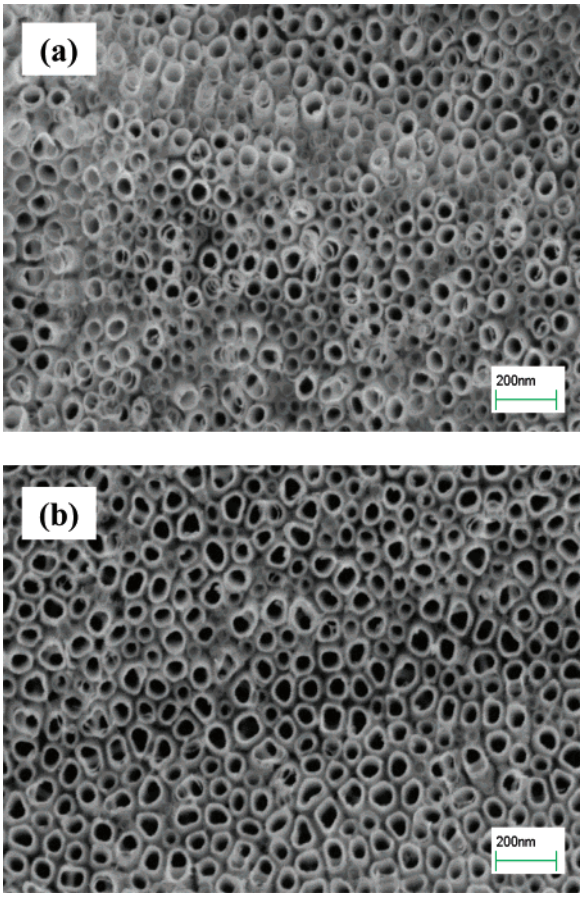

Figure 4. SEM images of TiO_2 nanotube arrays grown by pulse anodization (pulse duration: 16 s) in 0.36 M NH_4F electrolyte with glycerol containing 10% water at 20 V/0 V (a) and (b) at 20 V/−4 V pulse sequences.

variable ratios of Na^+/NH_4^+ (1:3, 1:1, and 3:1). Interestingly, replacement of NH_4^+ with Na^+ inhibited TiO_2 nanotube growth as seen by SEM. Even at a Na^+/NH_4^+ ratio of 1:3, no nanotube formation was noted under pulse anodization. Clearly, the protective (surface-passivating) effect of NH_4^+ is compromised by the presence of sodium ions at the interface. Presumably, even relatively small amounts of Na^+ in the electrical double layer suffice to counteract the favorable influence of NH_4^+ in ameliorating chemical attack of the oxide surface by the fluoride ions.

As in our companion studies,[1,14] the use of polyhydric alcohols (especially, ethylene glycol and PEG) for tuning the TiO_2 nanotube morphology is an innovative feature. The interfacial chemistry role of these alcohols and NH_3/NH_4^+ species was further probed by laser Raman spectroscopy. Figure 5 contains representative spectra for TiO_2 nanotube arrays grown by pulse anodization (20 V/−4 V); the oxide surface in each case had been in contact with the corresponding electrolyte bath in which it had been prepared, i.e., NH_4F/glycerol, NH_4F/ethylene glycol, and NH_4F/PEG 400. For comparison with these three spectra, a reference spectrum containing the TiO_2 lattice phonon modes is also shown as an insert in Figure 5. This particular reference sample was grown by conventional anodization (20 V, 3 h) in 0.36 M NH_4F/ethylene glycol.

Four Raman bands are clearly seen in the reference spectrum for the "clean" TiO_2 nanotube surface at 147, 385, 519, and 641 cm^{-1} and assigned to E_g, B_{1g}, E_{1g}, and E_g active modes, respectively, using reported reference spectra pertaining to the anatase TiO_2 structure.[28−30] No Raman bands related to the rutile phase are seen, as the rutile phase is characterized by bands at 143, 235, 447, and 612 cm^{-1}, respectively, which are not seen in this spectrum.[31] No significant broadening or shift were found when compared to the anatase TiO_2 powder. Observe that in the spectra for TiO_2 nanotubes after being in contact with the preparative electrolyte, the bands for anatase TiO_2 nanotubes are also clearly discernible although slightly shifted (<10−15 nm).

Particularly significant to note in the three spectra in Figure 5 are the bands assignable to the presence of NH_3/NH_4^+ species. Thus the band at 999.8 cm^{-1} is assigned to NH_3 by analogy with the theoretically predicated band for free ammonia at 964.3 cm^{-1}.[32] The band at 1228.0 cm^{-1} in NH_4F/glycerol is assignable to NH_3 (symmetric bending mode); this band is seen to shift to higher numbers when the coverage by ammonia on TiO_2 increases and was reported at 1220 cm^{-1} for TiO_2 anatase.[33] The bands at 1428 and 1480 cm^{-1} are assigned to the ammonium ion by comparison with similar bands located at 1415 and 1465 cm^{-1}, respectively, for the ammonium cation in NH_4SO_4.[34]

(28) Zhang, Y. H.; Chan, C. K.; Porter, J. F.; Guo, W. *J. Mater. Res.* **1998**, *13*, 2602.
(29) Bersani, D.; Lottici, P. P. *Appl. Phys. Lett.* **1998**, *72*, 73.
(30) Miao, L.; Tanemura, S.; Toh, S.; Kaneko, K.; Tanemura, M. *J. Crystal Growth* **2004**, *264*, 246.
(31) Zhang, J.; Li, M.; Feng, Z.; Chen, J.; Li, C. *J. Phys. Chem. B* **2006**, *110*, 927.
(32) Herzberg, G. *Infrared and Raman Spectra of Polyatomic Molecules*; Van Nostrand Reinhold: New York, 1945.
(33) Hadjiivanov, K.; Lamotte, J.; Lavally, J.-C. *Langmuir* **1997**, *13*, 3374.
(34) Jarawaia, M.; Crawford, J.; LeCaptain, D. J. *Ind. Eng. Chem. Res.* **2007**, *46*, 4900.

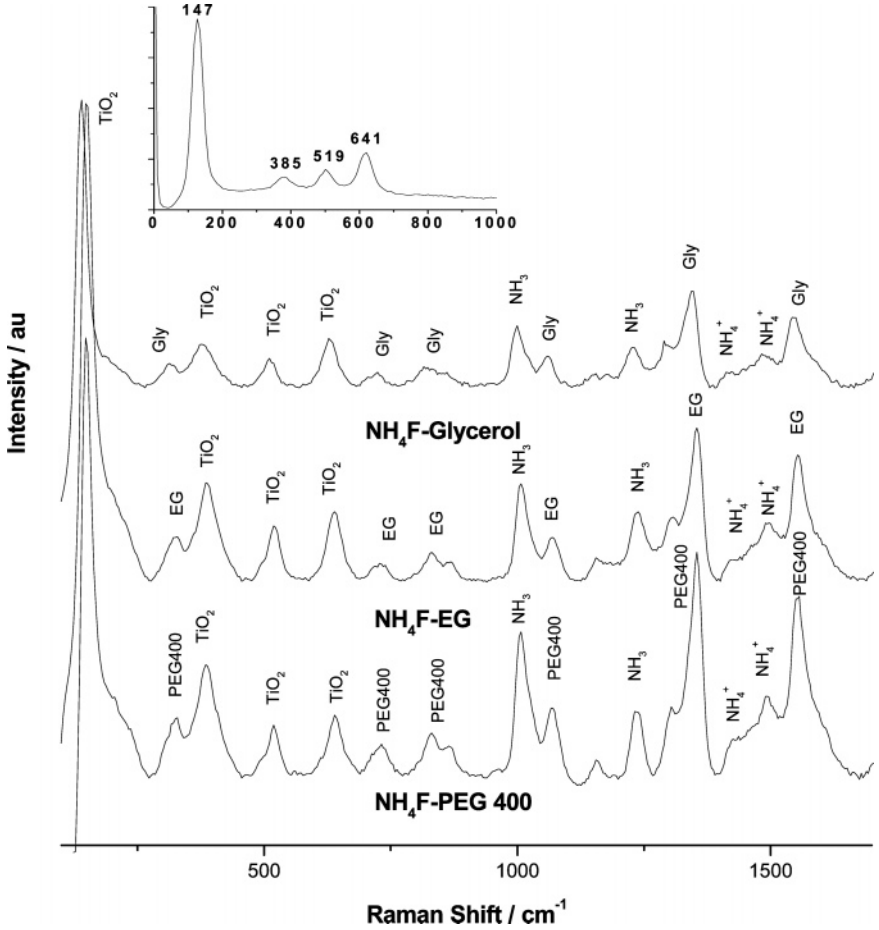

Figure 5. Raman spectra of TiO_2 nanotube arrays grown by pulse anodization (20 V/−4 V) in 0.36 M NH_4F/glycerol, 0.36 M NH_4F/ethylene glycol, and 0.36 M NH_4F/PEG 400 for 3 h, respectively. The spectra were obtained ex situ after the films were removed from the respective electrolytic bath and thermally annealed. For comparison, a reference spectrum of a TiO_2 film prepared with conventional anodization (20 V, 3 h) in 0.36 M NH_4F/ethylene glycol is included in the insert.

The Raman bands traceable to the three alcohols have a high degree of resemblance; for example, the δ(CC) is shown at 325.6 for adsorbed glycerol but slightly shifted to higher wavenumbers for ethylene glycol and PEG 400; the COH deformation appears at 1343.7 cm^{-1} for adsorbed glycerol and at 1354.5 cm^{-1} for both ethylene glycol and PEG 400. The CCO vibration modes appear at 1059.2 cm^{-1} and 1145 cm^{-1} for glycerol and at 1070.3 and 1157.3 cm^{-1} for the other two alcohols. The band at 1542.8 cm^{-1} in glycerol is tentatively assigned to $\delta(CH_2)$, appearing slightly shifted to 1553.3 cm^{-1} for ethylene glycol and PEG 400, although, in the latter, the band is significantly more intense when compared to the intensity of the TiO_2 signature bands. Finally, the three low-intensity bands in the 730−890 nm range are assigned to COC symmetric vibrations. These band assignments are supported by literature data on the three polyhydric alcohols.[35−37]

Effect of Pulse Duration. Figure 6a shows the surface morphology of a sample prepared by conventional anodization (20 V, 3 h) in 0.36 M NH_4F/ethylene glycol−H_2O (90:10). Individual groups of nanotube arrays are seen separated by big crevices as if uncontrolled chemical/electrochemical etching of the nanotube walls had occurred and the nanotube array formation was unable to develop on the entire substrate surface. There are apparent patches with nonporous structure and also some cloudy precipitates covering the surface. However, Figure 6b shows the surface morphology obtained under the same electrolytic conditions but with 20 V/0 V pulse anodization using the pulse duration $t_0 = 16$ s at the lower voltage limit. Large areas covered with the self-organized nanotube arrays and much less cloudy precipitate on top of the nanotube arrays were found compared to the previous case (cf., Figure 6a and b).

Anodization using shorter pulse duration ($t_0 = 7$ s) yielded well structured areas of nanotube arrays covering almost the entire surface (Figure 6c). The amount of precipitates on top of the self-organized nanotubes is negligible. Interestingly a much shorter pulse duration ($t_0 = 2$ s) gave a regular porous structure consisting of organized nanotubes with uniform single pore diameters of approximately 69−71 nm (Figure 6d). Further, nanotubes prepared by pulse anodization using short t_0 pulse durations were longer than those from longer t_0 and from a constant voltage mode (see Table 1). The related photocurrent data reflect this morphology (Table 1, column 8).

The current transients recorded during the formation of nanotube arrays depicted in Figure 6b−d are shown in Figure 1b with the corresponding three t_0 values indicated at the bottom right corner of each current profile. When the anodization voltage is applied, the current increases and reaches a steady level while the barrier layer is reaching a thickness correspond-

(35) Mendelovici, E.; Frost, R. L.; Kloporgge, T. *J. Raman Spectrosc.* **2000**, *31*, 1121.
(36) Djaoued, Y.; Robichaud, J.; Brüning, R.; Albert, A.-S.; Ashrit, P. V. *Mater. Sci.* **2005**, *23*, 15.
(37) Luo, R-S.; Jonas, J. *J. Raman Spectrosc.* **2001**, *32*, 975.

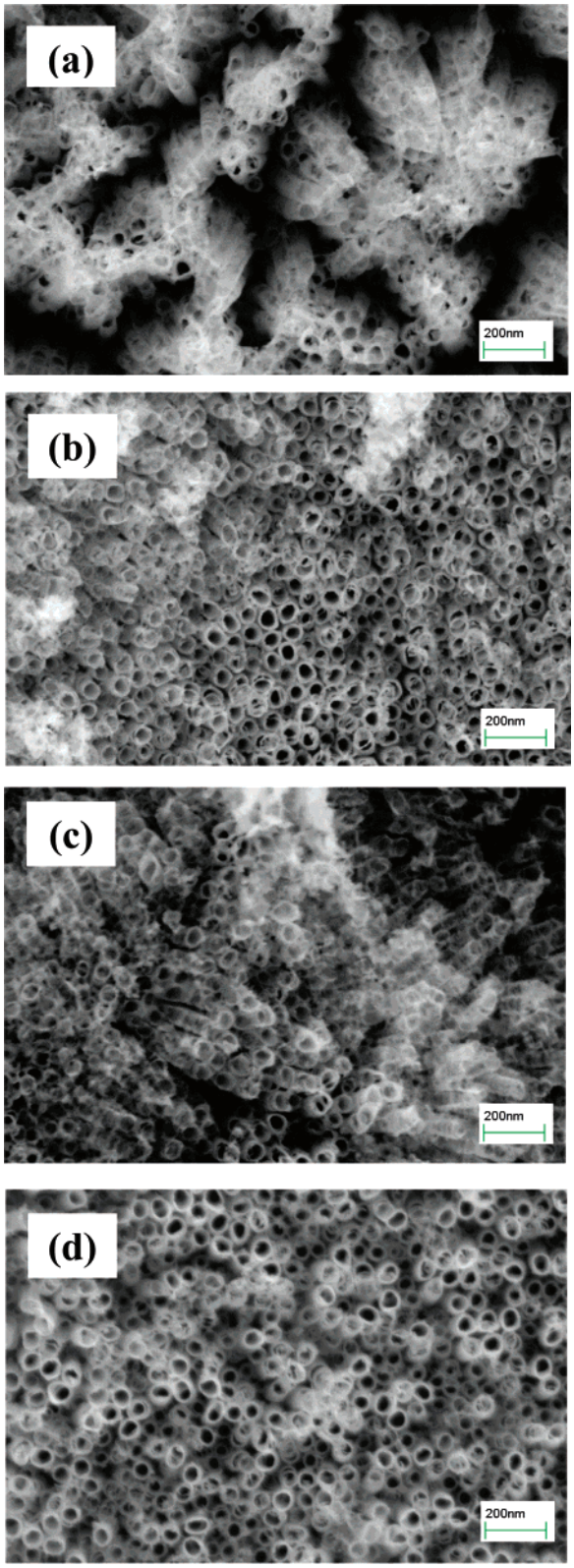

Figure 6. Comparison of SEM images of nanotube arrays of TiO_2 grown by conventional anodization (20 V, 3 h) in 0.36 M NH_4F/ethylene glycol (a) and by pulse anodization (20 V/0 V) with $t_0 = 16$ s (b), $t_0 = 7$ s (c), and $t_0 = 2$ s (d), respectively.

ing to nanotube formation. When the voltage is suddenly changed to the lower limit of the waveform the current density is seen to decrease drastically to very small values because the electrochemical growth/dissolution of the nanotube arrays are very low. Hence in this pulse period t_0, oxide formation is almost negligible, and the main processes in this period is the interaction of the growing nanotubes with F^- and NH_4^+ species, these two species affecting chemical dissolution of the oxide. When the voltage is again increased, the current density will reach a steady level and the oxide starts forming again.

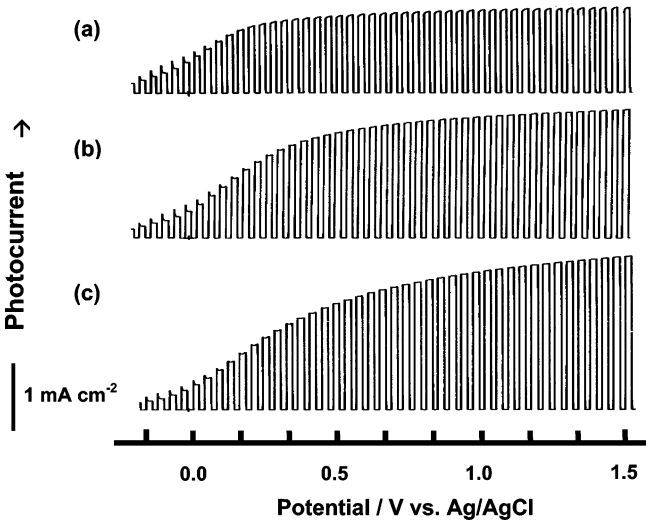

Figure 7. Linear-sweep photovoltammograms with 0.1 Hz chopped irradiation of a nanoporous TiO_2 film in 0.5 M Na_2SO_4. The films were obtained by conventional anodization (a) in 0.36 M NH_4F, 20 V for 3 h and (b) pulse anodization with $t_0 = 30$ s at −4 V/20 V in 0.36 M NH_4F, and (c) pulse anodization with $t_0 = 30$ s at −4 V/20 V in 0.36 M NH_4F/ PEG 400. Photovoltammograms were obtained at 2 mV/s using the full output of a 150 W Xe lamp.

Thus the formation of nanotubes will occur more slowly avoiding cracking of the surface. This also prevents the nanotubes from clumping together, as well as eliminating cloud formation on the nanotube surface from rapid oxide formation.[3] With 0 V as the lower potential of the waveform the effect of fluoride chemical dissolution is more marked than in the case of −4 V. Once again, a negatively polarized oxide film promotes the electrostatic attraction of NH_4^+ that in turn slows down the oxide being chemically etched by fluoride (see above).

Photoelectrochemical Performance. The photoelectrochemical response of the TiO_2 nanotube films was assessed using linear sweep photovoltammetry[38,39] in a 0.5 M Na_2SO_4 supporting electrolyte. Figure 7 shows representative photovoltammograms for TiO_2 nanotube arrays prepared by conventional anodization in 0.36 M NH_4F at 20 V for 3 h (entry 1, Table 1) (Figure 7a), nanotube arrays prepared by pulse anodization using pulse duration ($t_0 = 30$ s) at 20/−4 V for 3 h (entry 5, Table 1) (Figure 7b), and samples from pulse anodization ($t_0 = 30$ s) in 0.36 M NH_4F/ PEG 400 at 20/−4 V for 3 h (entry 29, Table 1) (Figure 7c).

The TiO_2 nanotubes grown by pulse anodization showed superior photovoltammetry profiles in both cases compared to their counterpart grown at constant anodization voltage. This trend reflects better $e^- - h^+$ pair separation and transport in the former cases. Clearly the nanoarchitecture morphology and

(38) Rajeshwar, K. In *Encyclopedia of Electrochemistry: Semiconductor Electrodes and Photoelectrochemistry*; Licht, S., Ed.; Wiley-VCH: Weinheim, Germany, 2002; Vol. 6, Chapter 1, pp 1−53.
(39) Zhou, M.; Lin, W.-Y.; de Tacconi, N. R.; Rajeshwar, K. *J. Electroanal. Chem*. **1996**, *402*, 221.

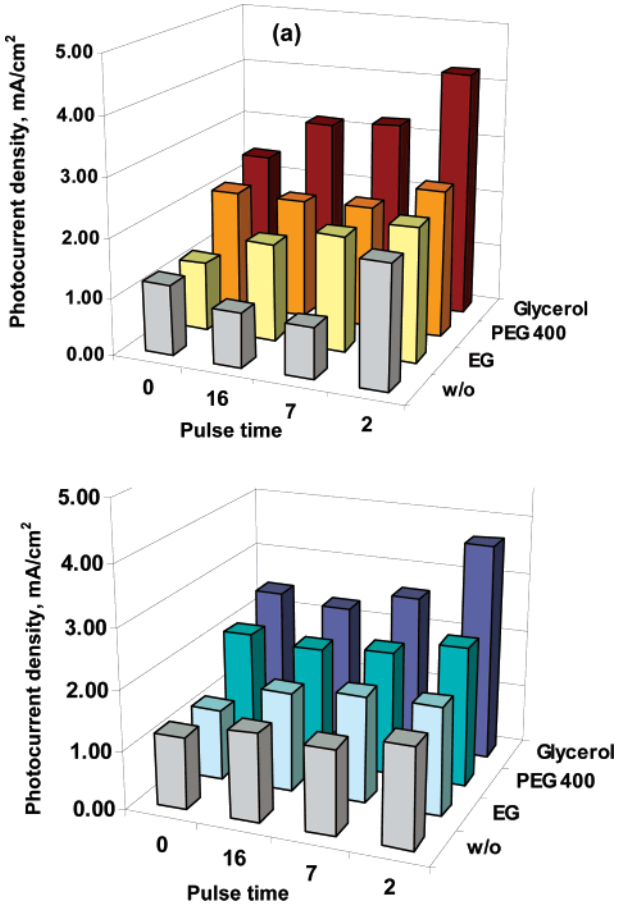

Figure 8. Bar graphs comparing photocurrent densities at a reverse bias potential of +1.5 V (vs Ag|AgCl reference) in 0.5 M Na_2SO_4 supporting electrolyte for films prepared without and with different media modifiers by conventional anodization (20 V, 3 h) and by pulse anodization for duration between 2 and 16 s at 20 V/−4 V (a) and 20 V/0 V (b).

photoresponse are directly linked underlining the rationale for using nanotube arrays in photoelectrochemical and solar energy conversion applications.

A figure-of-merit indicator of the quality of photoelectrochemical response is the photocurrent density value at the plateau region of the photovoltammograms (see Figure 8). Such values are contained in Table 1 (column 8). The photoelectrochemical response of TiO_2 films prepared under constant (20 V) and pulse (20 V/−4 V or 20 V/0 V) polarization are shown in Figure 8a and b, respectively. The data are shown in bar graph format comparing photocurrent densities for the various samples (at a reverse bias potential of +1.5 V vs Ag|AgCl reference in 0.5 M Na_2SO_4 supporting electrolyte) on the *z*-axis and pulse duration on the *x*-axis. The photocurrent densities are higher by ∼12% to ∼45% for the pulse (20 V/−4 V) anodized nanotube arrays relative to samples obtained from the conventional, continuous anodization approach and by ∼7% to ∼15% for pulse anodization at 20 V/0 V.

The lower photocurrent densities in films prepared by constant anodization are likely related to the fact that these films are made of thinner nanotube walls than those prepared by pulse anodization. These thinner walls imply that smaller amounts of charge are collected in the back contact because of two factors: slow charge transport through the walls and accelerated recombination due to a high concentration of injected electrons. There is precedence for the observation of lower photocurrent efficiency at thin nanotube walls (less than 5 nm) in ZnO nanotubular photoanodes grown in an anodic aluminum oxide template.[40]

Importantly, note in Figure 8a that the highest photocurrent in each medium modifier (glycerol, ethylene glycol and PEG 400) was obtained for a pulse duration of 2 s. Reference to Table 1 indicates that this pulse duration generates a comparable wall thickness with values of 15.6 ± 0.5 nm for glycerol and 15.4 ± 0.5 nm for both ethylene glycol and PEG 400. This finding suggests that a nanotube wall thickness of 15.5 nm is optimal for good photoelectrochemical performance.

In terms of the comparative effect of the three medium modifiers (glycerol, ethylene glycol, and PEG 400) on the resulting photoelectrochemical performance of TiO_2 nanotube arrays, those from glycerol perform the best for water photooxidation. These nanotubes have diameters ranging from 60 ± 2 nm to 83 ± 2 nm depending on the anodization waveform, and these dimensions seem optimal for not getting blocked by O_2 bubbles generated inside the tubes. Larger nanotube diameters such as those generated from PEG 400 do not perform better than those from glycerol. Thus the medium modifiers clearly play a role in the nanotube wall thickness, diameter, and length under different waveform potentials and durations (see Figure 3), and these variables, in turn, impact the photoelectrochemical response. The interfacial effect of these medium modifiers is not limited to solution viscosity changes.[6] The present study has clearly shown that polyhydric alcohols can interact with the growing oxide surface (Figure 5). Additionally, they can reduce the water activity in the growth medium. For example, glycerol and ethylene glycol have been used as water activity depressor agents.[41]

Importantly, the breakdown of organic solvent at the negative pulse limit could play an important role in nanotube formation and subsequent photoelectrochemical performance. In fact, there are clear differences in the photocurrent performance for films prepared using the same pulse waveform in the three polyhydric alcohols (see Figures 7 and 8). For example, for a pulse limit of −4 V (2 s), the three resulting films share similar nanotube wall thicknesses but the photocurrent is almost double for the film prepared from glycerol.

Conclusions

The present work focuses on the self-organized formation of TiO_2 nanotube arrays in different nonaqueous and aqueous organic polar electrolytes by pulse anodization with varying waveform profiles. The SEM morphology of the TiO_2 nanotubes indicates that nanotubes are formed in better self-organized arrays under pulse anodization than their counterparts grown at constant anodization voltage. This better nanotube morphology in turn translates to better photoelectrochemical response, the photocurrent densities for the nanotubes of TiO_2 films obtained by pulse anodization being significantly higher (up to 45%) than their counterparts grown at constant anodization voltage. In particular, this study has demonstrated that the pulse anodization mode adds another dimension to the tuning and optimization of nanotube characteristics for titanium substrate

(40) Martinson, A. B. F.; Elam, J. W.; Hupp, J. T.; Pellin, M. J. *Nano Lett.* **2007**, *7*, 2183.
(41) Chuy, S.; Bell, L. N. *Food Res. Int.* **2002**, *39*, 342.

surfaces. Specifically, choice of a negative pulse voltage limit (−4 V) serves to electrostatically bind NH_3/NH_4^+ species on the oxide surface and thus ameliorate the extent of its chemical attack by fluoride ions in the electrolyte. Better nanotube morphology in turn translates to better photoelectrochemical response. Besides, the simultaneous use of polyhydric alcohols (e.g., glycerol, ethylene glycol, PEG 400) in the anodization bath also serves to optimize nanotube formation and self-assembly as demonstrated in this study. Thus the data presented above show that pulse-anodized TiO_2 nanotube arrays will be eminently attractive candidates for solar photovoltaic conversion applications; studies oriented in this direction are in progress.

Acknowledgment. This research was supported in part by a grant from the U.S. Department of Energy (Office of Basic Energy Sciences). We thank Eugenio Tacconi for the kind donation of the multioutput power supply, and K. R. thanks the University of Texas System for a STARS grant. Finally, the three anonymous reviewers are thanked for constructive criticisms of an earlier manuscript version.

JA076092A